

# Penetration of intense charged particle beams in the outer layers of precompressed thermonuclear fuels

C. DEUTSCH

Laboratoire de Physique des Gaz et Plasmas, (CNRS-UMR), Université Paris XI,  
ORSAY Cedex, France

(RECEIVED 30 May 2003; ACCEPTED 31 August 2003)

## Abstract

This paper emphasizes the energy dissipation through collective electromagnetic modes (mostly transverse to the incoming beam) of ultraintense relativistic electrons and nonrelativistic protons interacting with a supercompressed core of deuterium + tritium (DT) thermonuclear fuel. This pattern of beam–plasma interaction documents the fast ignition scenario for inertial confinement fusion.

The electromagnetic Weibel instability is considered analytically in a linear approximation. Relevant growth rate parameters then highlight density ratios between target and particle beams, as well as transverse temperatures. Significant refinements include mode–mode couplings and collisions with target electrons. The former qualify the so-called quasi-linear (weakly turbulent) approach. Usually, it produces significantly lower growth rates than the linear ones. Collisions enhance them slightly for  $k_c/\omega_p < 1$ , and dampen them strongly for  $k_c/\omega_p \geq 1$ . Those results simplify rather drastically for the laser-produced and nonrelativistic proton beams. In this case, those growth rates remain always negative through a wide range of beam–target parameters.

**Keywords:** Fast ignition; Quasi-linear treatment; Weibel instability

## 1. INTRODUCTION

The recently proposed fast ignitor (FIS; Tabak *et al.*, 1994) designed for monitoring the ignition process within any inertial confinement fusion (ICF) scheme highlights to the extreme, the splitting paradigm of cheap compression through MJ drivers (heavy ions, lasers) followed by the expensive triggered ignition of the compressed fuel with petawatt lasers. The latter are first expected to bore a hole in the corona of the compressed DT core, and also to produce with a good efficiency intense relative electron beams (REB) at megaelectron volt levels, through critical surface crushing (Lefebvre & Bonnaud, 1995). This latter feature has been indeed positively documented through numerical simulations and laser firing of thin cold foils. It thus remains to witness a successful penetration of those intense REB through steep density gradients ranging from  $10^{21}$  e/cm<sup>3</sup> in the corona down to  $10^{26}$  e/cm<sup>3</sup> in the DT core at a 100  $\mu$ m or so distance. FIS has already received much attention, and its

best understood steps include the ponderomotive laser penetration in the corona as well as the in depth hot spot building up through REB interacting inelastically with target electrons and also experiencing multiple (mostly elastic) scattering on target ions (Deutsch *et al.*, 1996). The latter processes hopefully combine to yield a hot spot with a 10- $\mu$ m extension for megaelectron volt REB. Intermediate steps are much more difficult to assert and remain a matter for intense scrutiny as well as hot contradictory debates (Honda, 2000; Honda *et al.*, 2000; Hain & Mulser, 2001).

This situation motivates the present inquiry into every collective mode produced in the REB dense core interaction that may eventually divert into a large volume the REB kinetic energy. It turns out that the most dangerous ones arise from the filamentation (Weibel) instability due to the overall electron distribution built on direct and return current as well. The anisotropy of the latter acts as a permanent source of entropy. We demonstrate that Weibel (transverse electromagnetic) is at its worst when REB density is close to critical. However, this instability that pervades every beam–target interaction scheme of ICF interest may nevertheless be mitigated through a transverse temperature gradient. In the final FIS phase,  $T_{lb} \sim 150$  eV seems sufficient. Then, we display results (see Fig. 1) of a three-dimensional (3D) PIC

Address correspondence and reprint requests to: C. Deutsch, Laboratoire de Physique des Gaz et Plasmas (CNRS-UMR No. 8578), Bâtiment 210, Université Paris XI, 91405 ORSAY Cedex, France. E-mail: claude.deutsch@lpgp.u-psud.fr

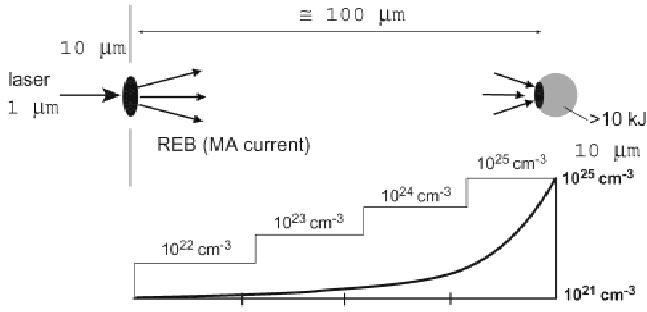


**Fig. 1.** Relativistic electron beam (REB) propagation with megaelectron volt incoming energy through layers of increasing density  $N_p$  in a core of precompressed DT fuel.

simulation supporting the view that collective effects monitor the REB–target interaction in the corona, while individual electron collisions take the lead with increasing core densities. In this respect, we supplement former REB stopping calculations (Deutsch *et al.*, 1996) with enhanced contributions arising from correlated and relativistic electron stopping for projectiles pairs with interdistances orders of magnitude larger than the target electron screening length (Deutsch & Fromy, 1999, 2000).

## 2. LINEAR AND QUASI-LINEAR WEIBEL GROWTH RATES

Exponential growth of linear transverse Weibel instability could be highly detrimental to the REB stopping in the outer layers of a DT precompressed core.

The linear stage plays a crucial role in initiating the transverse and deleterious further filamentation process that could divert a substantial amount of REB energy initially intended to be deposited in the precompressed DT target.

### 2.1. Relativistic e-beams

Very recent experimental results seem to confirm the relative electron beams (REB) penetration in dense and hot plasmas with parameters compatible with those of possible outer layers surrounding a superdense DT core (see Fig. 1; Kodama *et al.*, 2001).

Such a situation motivates our present focus on the basic mechanisms affecting REB propagation during the initial time scale  $\sim \omega_p^{-1}$  ( $\omega_p$  is the target plasma frequency) when Weibel electromagnetic instability (WEI) behaves mostly linearly. In particular, we intend to stress the N-body features of REB stopping in those specific conditions.

For our purposes, we find it useful to start with a collisional formulation of the Vlasov equation with a Krook term (Okada & Niu, 1980) in the right-hand side, that is,

$$\frac{\partial f}{\partial t} + \mathbf{v} \cdot \frac{\partial f}{\partial \mathbf{r}} + q \left( \mathbf{E} + \frac{\mathbf{v}}{c} \times \mathbf{B} \right) \cdot \frac{\partial f}{\partial \mathbf{p}} = -\nu(f - f_0), \quad (1)$$

where  $\nu$  is the effective collision frequency,  $f$  is the electron distribution function at position  $\mathbf{r}$  and momentum  $\mathbf{p}$  at time  $t$ ,  $f_0$  is the distribution function,  $q$  denotes the charge (including sign),  $c$  is light speed,  $\mathbf{v}$  and  $\mathbf{p}$  are related by  $\mathbf{v} = \mathbf{p}/m\gamma$ ,  $\gamma_b = (1 + p^2/(mc)^2)^{1/2}$  and  $m$  is the electron rest mass.

Let us now consider a current neutral beam–plasma system. The relativistic electron beam propagates with the velocity  $\mathbf{V}_d^b$  and the plasma return current flows with  $\mathbf{V}_d^p$ . It is reasonable to assume that an electromagnetic mode has  $\mathbf{k}$  normal to  $\mathbf{V}_d^b$ , perturbed electric field  $\mathbf{E}$  parallel to  $\mathbf{V}_d^b$ , and perturbed magnetic field  $\mathbf{B}$  normal to both  $\mathbf{V}_d^b$  and  $\mathbf{E}$ . So, the total asymmetric  $f_0$  consist of nonrelativistic background electrons and relativistic beam electrons:

$$f_0(\mathbf{p}) = \frac{n_p}{2\pi m (\theta_x^p \theta_y^p)^{1/2}} \exp\left(-\frac{(p_x + p_d^p)^2}{2m\theta_x^p} - \frac{p_y^2}{2m\theta_y^p}\right) + \frac{n_b}{2\pi m \gamma (\theta_x^b \theta_y^b)^{1/2}} \exp\left(-\frac{(p_x + p_d^b)^2}{2m\gamma\theta_x^b} - \frac{p_y^2}{2m\gamma\theta_y^b}\right). \quad (2)$$

Here  $\theta_x, \theta_y$  are the temperature components parallel to the  $x$  and  $y$  directions,  $\mathbf{p}_d$  is the drift momentum, and superscripts  $p$  and  $b$  represent the plasma electron and the beam electron, respectively. From the linearized Vlasov equation with the collision term (1) and linearized Maxwell's equations we get the linear dispersion relation for a purely transverse graving mode fulfilling

$$1 + \chi_p^L(k, \omega) + \chi_b^L(k, \omega) = k^2 c^2 / \omega^2, \quad (3)$$

$$\chi_p^L(k, \omega) = \frac{\omega_p^2}{\omega(\omega + i\nu)} \left[ 1 - AW(\xi) - \frac{i\nu}{\omega} (A - 1)W(\xi) \right], \quad (4)$$

$$\chi_b^L(k, \omega) = \frac{\omega_b^2}{\omega^2} [1 - BW(\eta)], \quad (5)$$

where

$$\omega_b^2 = 4\pi n_b q^2 / m\gamma_b, \quad \omega_p^2 = 4\pi n_p q^2 / m,$$

denote beam and target electron plasma frequency and

$$A = (\theta_x^p + p_d^{p2}/m) / \theta_y^p$$

$$B = (\theta_x^b + p_d^{b2}/m\gamma_b) / \theta_y^b$$

refer to corresponding asymmetry parameters, with

$$\xi = (\omega + i\nu) / k \sqrt{(\theta_y^p/m)}$$

and

$$\eta = \omega / k \sqrt{(\theta_y^b/m\gamma_b)}.$$

$\chi_p^L$  is the plasma linear susceptibility and  $\chi_b^L$  that for the beam.

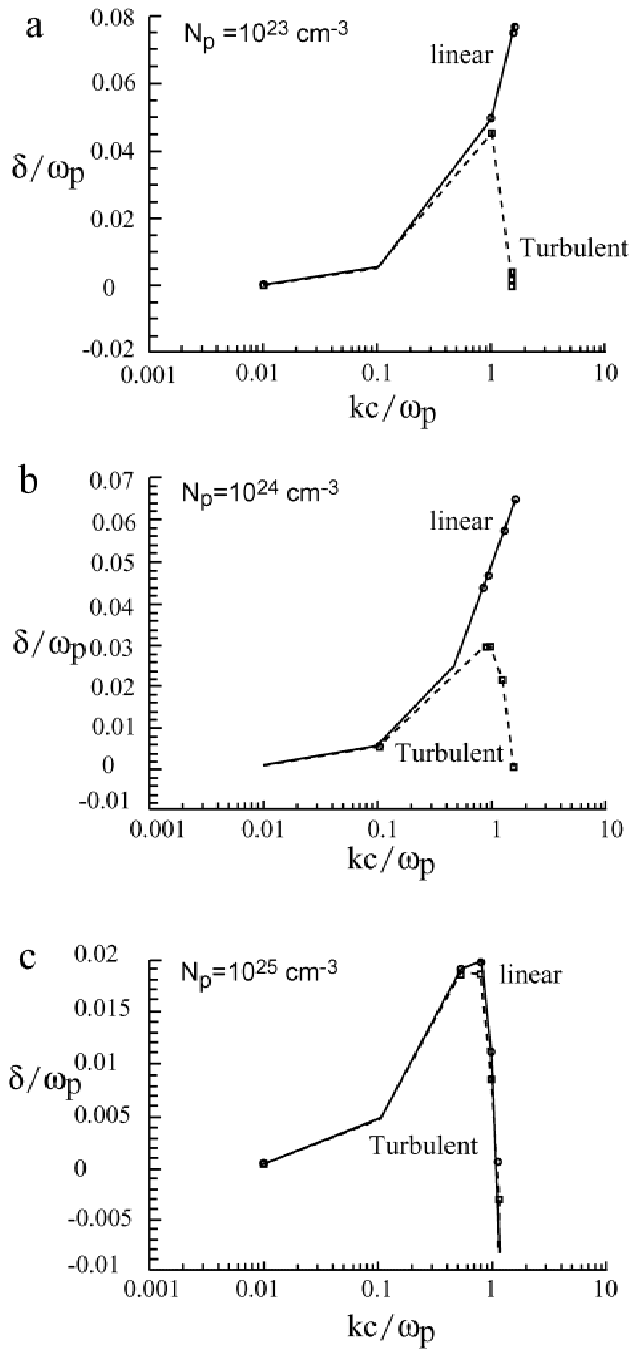


**Fig. 2.** Linear and quasi-linear (“turbulent”) WEI growth rates in a DT plasma with  $T_p = 100$  eV at increasing  $N_p$ . (a)  $10^{23}$   $\text{cm}^{-3}$ , (b)  $10^{24}$   $\text{cm}^{-3}$ , and (c)  $10^{25}$   $\text{cm}^{-3}$ .  $E_b = 1$  MeV and  $T_b = 1$  keV.

We restrict consideration of collisional effect to the background plasma and assume a weak beam ( $\omega_b < \omega_p$ ). The function  $W(z)$  is taken in the usual Fried–Conte form as

$$W(z) = (2\pi)^{-1/2} \int_{-\infty}^{\infty} \frac{y}{y-z} \exp\left(-\frac{1}{2}y^2\right) dy. \quad (6)$$

Paying attention to the WEI linear growth rate (LGR), we notice that this LGR is essentially controlled by the two

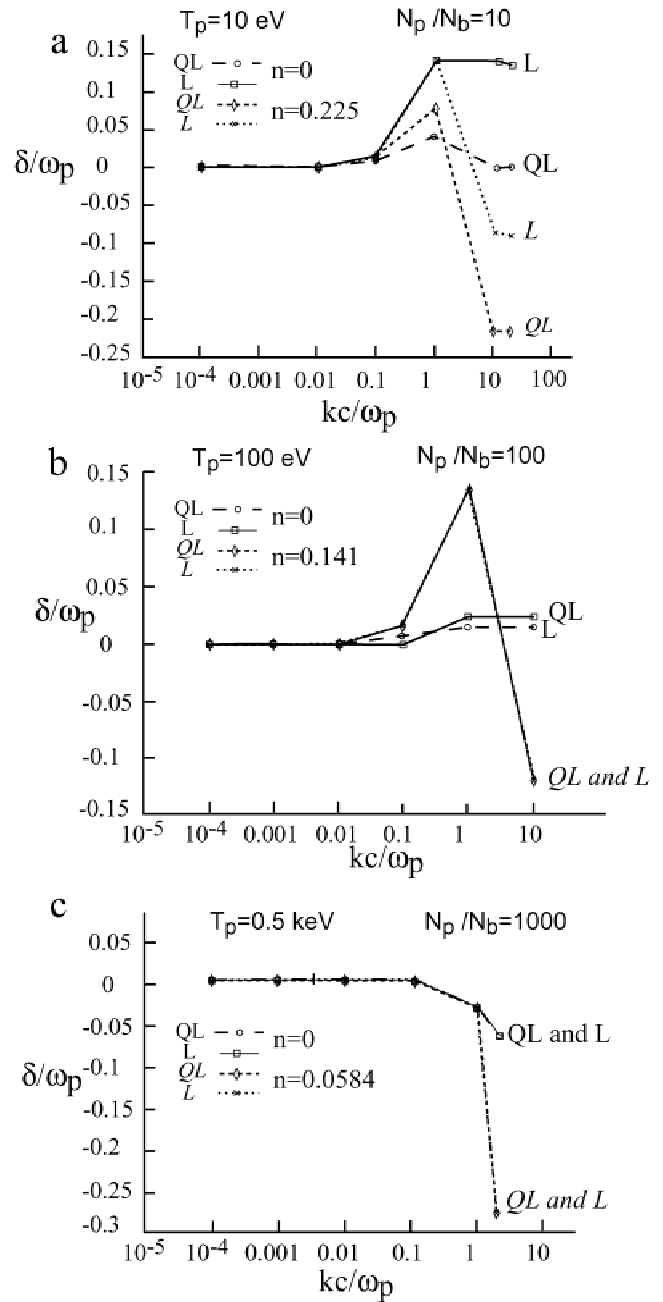


**Fig. 3.** Weibel growth rates for a REB with anisotropic temperature  $T_b$  (ortho,para) = 10 keV, 10 eV, density  $N_b = 10^{22}$   $\text{cm}^{-3}$  and energy  $E_b = 1$  MeV in target electron. Plasma with (a)  $T_p = 10$  eV,  $N_p/N_b = 10$ ; (b)  $T_p = 100$  eV,  $N_p/N_b = 500$ ; (c)  $T_p = 1$  keV,  $N_p/N_b = 1000$ ;  $n = \nu/\omega_p$  qualifies a REB target collision rate.

asymmetry parameters:

$$A = 1 + r^2 511(1 - \gamma_b^{-2})T_p^{-1},$$

$$B = 1 + 511(\gamma_b - \gamma_b^{-1})T_b^{-1}, \quad (7)$$

obtained below Eq. (5), where  $r = n_b/n_p$ ,  $T_b$  and  $T_p$  denote, respectively, REB and target plasma isotropic temperature in kiloelectron volts.  $V_p$  denotes REB velocity.

Moreover, it is also useful to remark that the quasi-linear theory (Dupree–Weinstock; Kono & Ichikawa, 1973) based on mode–mode coupling can provide even more accurate parameters, in the form

$$A' = \frac{AT_p}{T_p + XD}, \quad B' = \frac{BT_b}{T_b + XD}, \quad (8)$$

with  $X$ , positive solution of  $(u = (rv_b/\gamma_b)^2)$ ,

$$(1 + r^2)X^4 + \left[ r^2 \frac{T_p}{m} + \frac{T_b}{m\gamma} (1 + r^2) \right] X^2 - u \left[ \frac{T_p}{m} + \frac{T_b}{m\gamma} \left( u^2 - r^2 \frac{T_p}{m} \right) \right] = 0 \quad (9)$$

and  $D = 511r(1 - \gamma_b^{-1})$  in kiloelectron volts. Using (A,B) and (A',B') in the relevant linear dispersion relations, we obtain the WEI growth rates depicted in Figure 2, as linear and turbulent, respectively. We then emphasize moderately hot ( $T_p = 100$  eV) outer DT layers and 1-MeV REB with a thermal  $T_b = 1$  keV. Maximum LGR  $\delta_{\max}$  occurs close to the skin depth wavelength  $c/\omega_p$ .  $\delta_{\max}$  is also shown steadily decaying with increasing  $N_p$ . Also, quasi-linear (“turbulent”) LGR profiles stand beneath linear ones.

In this connection, it is useful to recall that collisional REB stopping increases nearly linearly with  $N_p$ . So, a figure of merit probing the relative importance of collective WEI energy dissipation of the REB against collisional stop-

ping is the e-folding number

$$N_{\text{efold}} = \delta_{\max} T_{\text{stop}}, \quad (10)$$

with

$$T_{\text{stop}} = \frac{1}{c} \int_{E_b^{\min}}^{E_b^{\max}} \frac{1 + \frac{E_b}{m_e c^2}}{\left[ \left( \frac{E_b}{m_e c^2} \right) \left( \frac{E_b}{m_e c^2} + 2 \right) \right]^{1/2}} \times \frac{dE_b}{dx}. \quad (11)$$

The evaluation of expression (5) is conveniently performed with the steplike  $N_p$  profile given in Fig. 1.  $E_b^{\max}$  and  $E_b^{\min}$  refer to extreme  $N_p$  values in every slab (25  $\mu\text{m}$  thick) with a fixed  $N_p$  in it, building up this profile in terms of the standard  $dE_b/dx$  Fermi expression for the relativistic stopping of a single electron projectile (Fermi, 1940).

### 2.2. Collisions contribution

In view of the very high densities reached by the precompressed pellet, it seems rather mandatory to pay attention to collisions between e-beam and target ions. Very often, these contributions are neglected in many standard treatments of the Weibel instability. A large consensus even asserts that collisions remain helpless against transverse electromagnetic growth rates. Nonetheless, no one has already given ground to the validity of such a claim in the present extreme situation we are now considering. To clear up this point, we

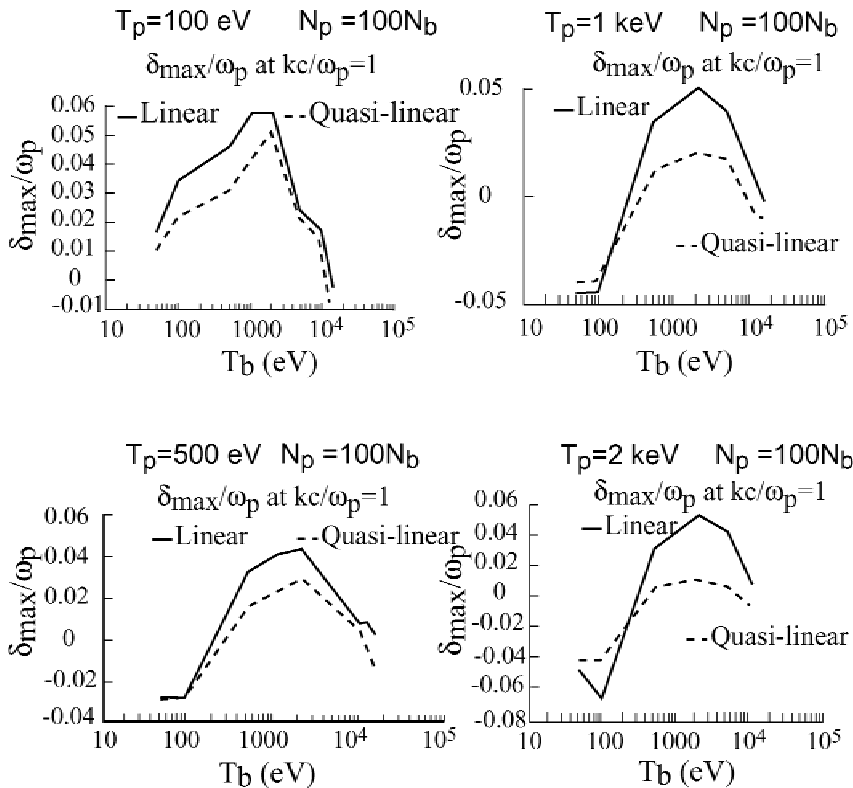


Fig. 4. Maximum REB growth rates at  $kc/\omega_p = 1$  with  $N_b = 10^{22} \text{ cm}^{-3}$  and  $E_b = 1 \text{ MeV}$ , in terms of isotropic  $T_b$ .  $N_p = 100 N_b$ .

included in the present treatment, a Krook collision term with the right-hand side of the corresponding Vlasov equation.

A few salient results are thus detailed in Figure 3a,b,c for the successive density slices featured in Figure 1.

The isotropic target temperature is taken to be systematically larger than the corresponding Fermi  $T_F$  accounting for nonnegligible quantum effects. We see that as target electron density increases from  $10^{23}$  up to  $10^{25}$   $\text{cm}^{-3}$ , the discrepancy between linear  $L$  and quasilinear  $QL$  growth rates progressively disappear. Also, collision-corrected growth rates  $\delta$  have a tendency to rise above the collisionless ones for  $10^{-2} \leq kc/\omega_p \leq 1$ . However, only the collision-corrected ones abruptly decay to negative (stabilization) values for  $1 \leq kc/\omega_p \leq 10$ . So, even in this rather extreme case of transverse electromagnetic instability, the beam–target collisions assert their usual damping role, as a priori expected on empirical grounds.

### 2.3. Maximum growth rates

A significant figure of merit for the growth rate of the transverse electromagnetic mode is obviously its maximum value for a wavelength target skin depth  $kc/\omega_p \cong 1$ . It is documented in Figure 4a–c for several isotropic target temperatures in terms of REB transverse temperature. A typical target density  $N_p = 100N_b$ , is selected. Whatever  $T_p$ , the given maximum growth rates display similar profiles with a maximum value around  $T_b \sim 1$  keV. It is quite suggestive that  $\delta$  is at minimum for very low or very high  $T_b$ . Another encouraging result is afforded by the quasi-linear profiles, lying systematically beneath the linear ones. Those quasi-linear profiles are also significantly lowering with increasing  $T_p$ .

### 3. NONRELATIVISTIC PROTONS

Increasing only projectiles energy  $E_b$  yields a significant growth rate increase for the WEI (former presentation). So, one is led to minimize  $\delta$  by reducing beam velocity, while still retaining a sufficient  $E_b$  for fast ignition. Those contradictory requirements may be fulfilled by turning to the recently unraveled and laser-produced proton beams (Roth *et al.*, 2001) in the 5–70 MeV energy range, with a 10% yield.

So, extending the present WEI quasilinear analysis to those projectiles, we picture in Figure 5a–c corresponding  $\delta_{\text{max}}$  values. Those latter turn always negative. A full  $\delta$  profile (Fig. 6) with temperatures of operational pertinence indeed confirm those statements.

Present quasilinear WEI growth rate demonstrates that beam and target densities, as well as respective transverse temperatures, are again the key parameters qualifying beam–plasma interactions of FIS concern.

High  $T_b$  and  $T_p$  values for  $N_b/N_p < 0.1$  should easily allow  $N_{\text{efold}} \leq 5$ , an acceptable figure. In every target plasma slab, one witnesses  $T_{\text{stop}} < 10^{-13}$  s for REB and  $T_{\text{stop}} < 10^{-12}$  s for protons.

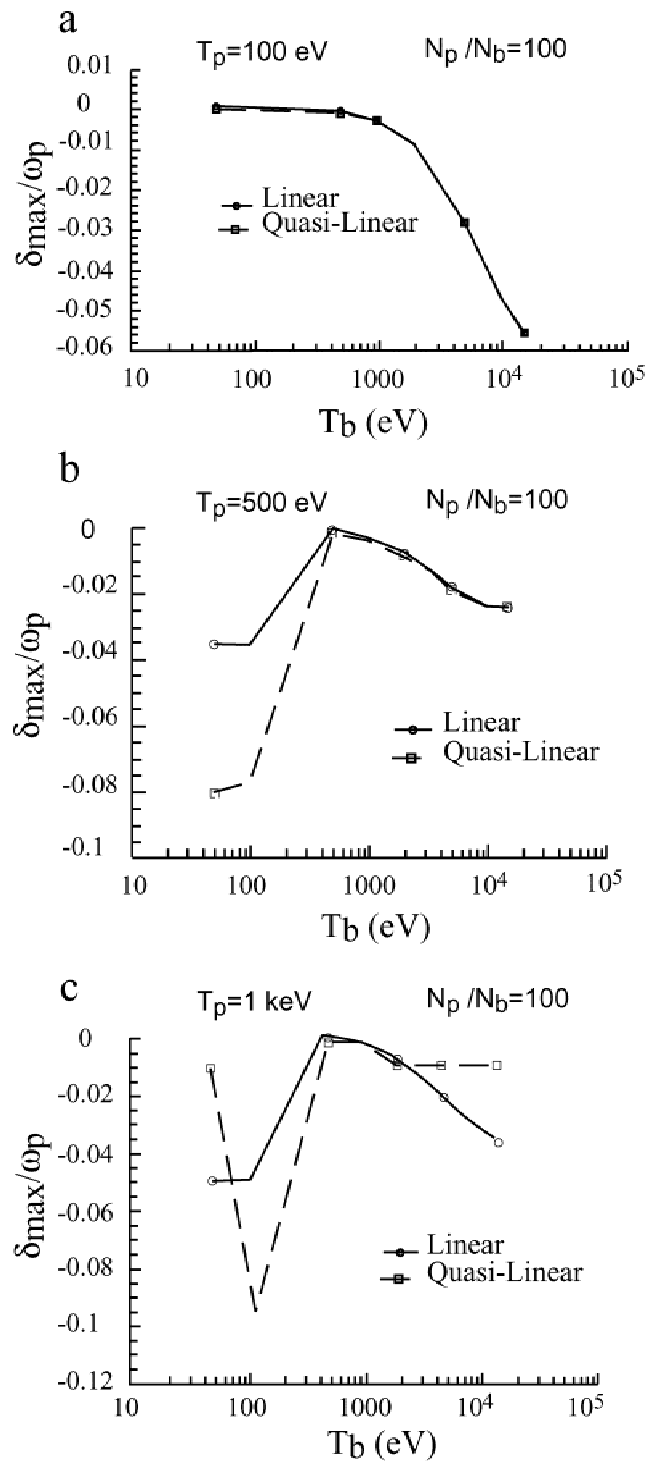


**Fig. 5.** Maximum Weibel growth rates at  $kc/\omega_p = 1$ , for 25 MeV protons with  $N_b = 10^{22}$   $\text{cm}^{-3}$  and isotropic  $T_p = 1$  keV.  $N_p = 100 N_b$ . Quasi-linear profiles are contrasted to linear ones.

So, a number of WEI e-foldings below 5 implies  $\delta_{\text{REB}}/\omega_p \leq 10^{-3}$  and  $\delta_{\text{proton}}/\omega_p \leq 10^{-4}$ . Those inequalities are indeed achievable in the context of present inertial fusion technology.

These considerations support the view that in outer DT layers with  $T_p < 5$  keV, most of the REB kinetic energy is

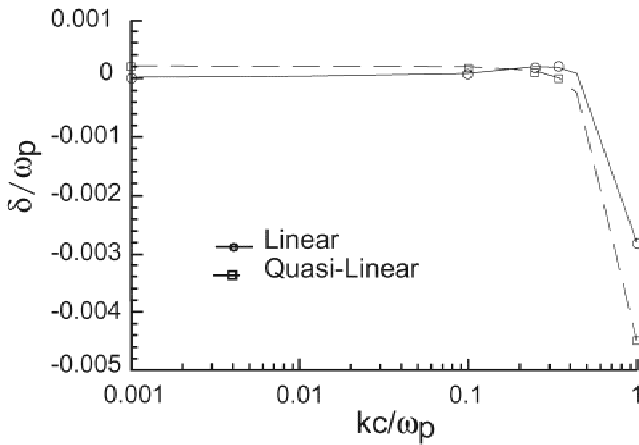


**Fig. 6.**  $\delta/\omega_p$  for 25-MeV protons in a target plasma with  $N_p = 10^{24} \text{ cm}^{-3}$ ,  $= 100N_b$ ,  $T_p = T_b = 1 \text{ keV}$ .

still dissipated through short-ranged electron–electron collisions and plasmon excitation documenting standard REB stopping in dense hot classical plasmas.

Once the crucial  $N_p = 10^{23} \text{ cm}^{-3}$  slab has been penetrated, the relative  $N_p$  increase of REB stopping versus WEI growth rates, on a time scale  $\sim \omega_p^{-1}$ , allows the electron projectiles to make their way in depth easily toward the DT core and trigger the hot spot through a kilojoule of local energy deposit.

In summary, we have demonstrated through a simple but efficient analytical modeling of the laser-produced REB interacting with outer and thus less dense layers of the supercompressed DT core that the initial in-depth propagation phase of the REB within the fast ignitor scenario could be effective on a time scale afforded by the linear growth of the electromagnetic instability.

Those considerations are even more appropriate for nonrelativistic proton beams that might offer the best option for driving fast ignition, provided their laser efficiency could be increased above 20%.

## REFERENCES

- DEUTSCH, C. & FROMY, P. (1999). Correlated stopping of relativistic electrons in superdense plasmas. *Phys. Plasmas* **6**, 3597–3606.
- DEUTSCH, C., FURUKAWA, H., MIMA, K., MURAKAMI, M. & NISHIHARA (1996). Interaction physics of the Fast ignitor concept. *Phys. Rev. Lett.* **77**, 2483–2486. Erratum (2000). **85**, 1140.
- FERMI, E. (1940). The ionization loss in gases and in condensed materials. *Phys. Rev.* **57**, 485–493.
- HAIN, S. & MULSER, P. (2001). Fast ignition without hole boring. *Phys. Rev. Lett.* **86**, 1015–1018.
- HONDA, M. (2000). On the maximum current for a self-focusing relativistic electron beam. *Phys. Plasmas* **7**, 1605–1606.
- KODAMA, R., NORREYS, P.A., MIMA, K., DANGOR, A.E., EVANS, R.G., FUJITA, H., KITAGAWA, Y., KRUSHELNIK, K., MIYAKOSHI, T., MIYANADA, N., NORMATSU, T., ROSE, S.J., SHOZAKI, T., SHIGEMORI, K., SUNAHARA, A., TAMPO, M., TANAKA, K.A., TOYAMA, Y., YAMANAKA, T. & ZEPF, M. (2001). Fast heating of ultrahigh-density plasma as step towards laser fusion ignition. *Nature* **412**, 798–802.
- KONO, M. & ICHIKAWA, Y.H. (1973). Renormalization of the wave-particle interaction in weakly turbulent plasmas. *Prog. Theor. Phys.* **49**, 754–763.
- LEFEBVRE, E. & BONNAUD, G. (1995). Transparency/opacity of a solid target illuminated by an ultrahigh-intensity laser pulse. *Phys. Rev. Lett.* **74**, 2002–2005.
- OKADA, T. & KIU, K. (1980). Electromagnetic instability and stopping power of plasma for relativistic electron beams. *J. Plasma Phys.* **23**, 423–432.
- ROTH, M., COWAN, T.E., KEY, M.H., HATCHETT, S.P., BROWIN, G., FOUNTAIN, W., JOHNSON, J., PENNINGTON, D.M., SNAVELY, R.A., WILDS, S.G., YASUIKE, K., RUHL, H., PEGORARO, F., BULANOV, S.V., CAMPBELL, E.M., PETTY, M. & POWELL, H. (2001). Fast ignition by intense laser-accelerated proton beams. *Phys. Rev. Lett.* **86**, 436–439.
- TABAK, M., HAMMER, J., GLINKSY, M.E., KRUEER, W.L., WILKS, S.C., WOODWORTH, J., CAMPBELL, M.E., PERRY, M.D. & MASON, R.J. (1994). Ignition and high gain with ultra powerful lasers. *Phys. Plasmas* **1**, 1626–1634.